

# PNAS

[www.pnas.org](http://www.pnas.org)

Supplementary Information for

Advanced fluorescence microscopy reveals disruption of dynamic CXCR4 dimerization by subpocket-specific inverse agonists

Ali İşbilir Jan Möller, Marta Arimont, Vladimir Bobkov, Cristina Perpiña-Viciano, Carsten Hoffmann, Asuka Inoue, Raimond Heukers, Chris de Graaf, Martine J. Smit, Paolo Annibale\*, Martin J. Lohse\*

\* Corresponding authors: Paolo Annibale and Martin J. Lohse

Email: [paolo.annibale@mdc-berlin.de](mailto:paolo.annibale@mdc-berlin.de), [lohse@toxi.uni-wuerzburg.de](mailto:lohse@toxi.uni-wuerzburg.de), [m.lohse@mdc-berlin.de](mailto:m.lohse@mdc-berlin.de)

**This PDF file includes:**

Figures S1 to S10  
Tables S1 to S3

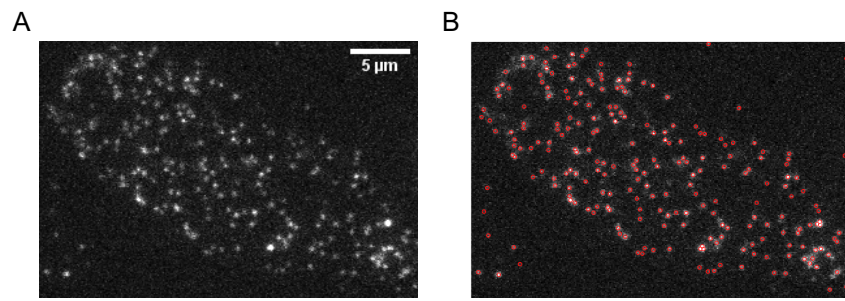


**Figure S1: Analysis of single particles from TIRF images. (A and B)** Single TIRF images of intact CHO cells expressing SNAP-CXCR4 labeled with SNAP-Surface 549 (A). Red spots around fluorescent particles represent that the particle was successfully recognized by the u-track software, with negligible recognition of unspecific particles outside of the cell (B).

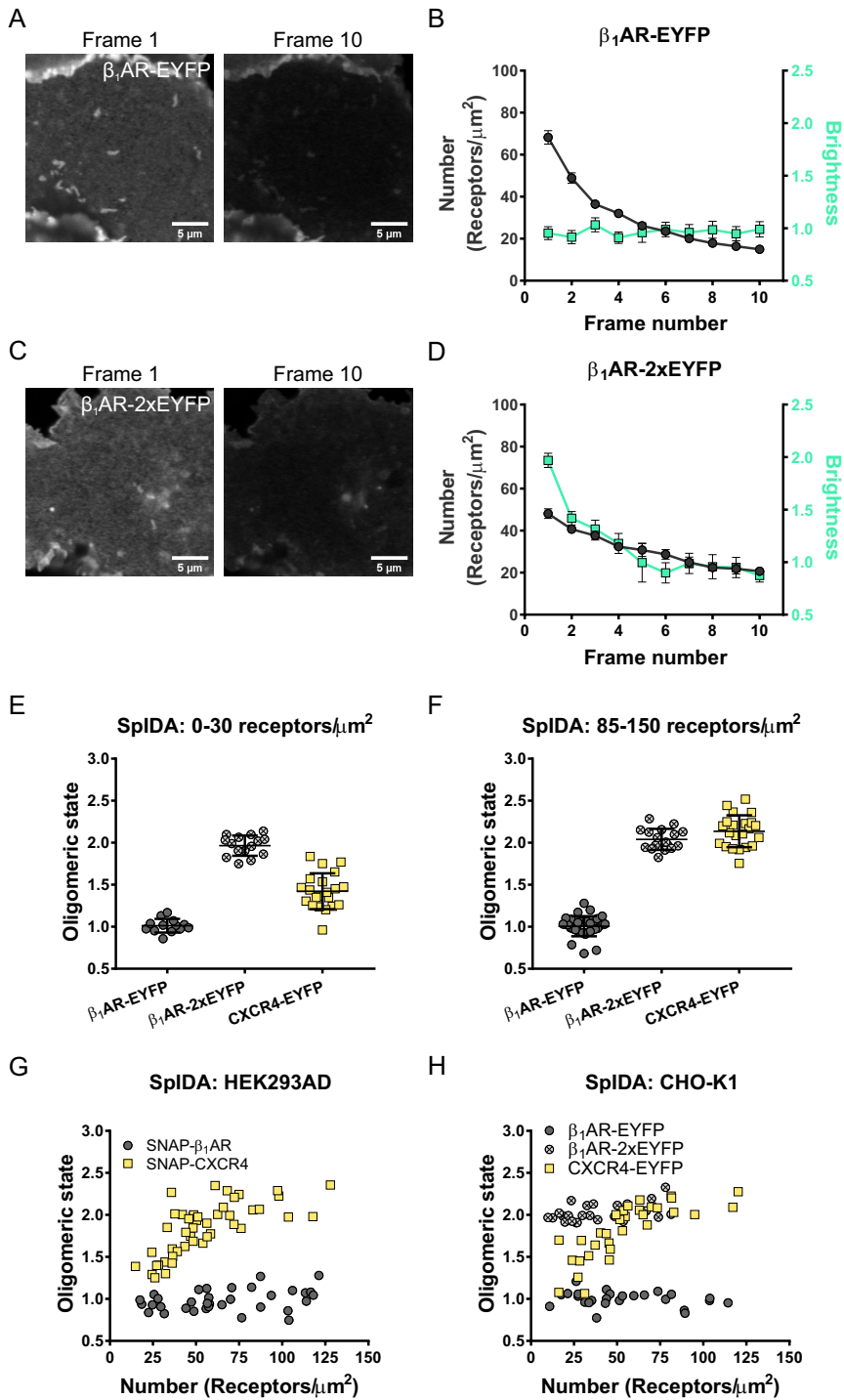


**Figure S2: SpIDA monomer/dimer controls characterization and CXCR4 density-dependent dimerization.** (A and C) First and last confocal images of single cells expressing  $\beta_1\text{AR-EYFP}$  (A) and  $\beta_1\text{AR-2xEYFP}$  (B) that are used for brightness and density calculation. Images are represented with the same brightness and contrast values to visualize photobleaching. (B and D) Time-course plot of brightness and density of the time-series images from (A) and (C). Despite  $\beta_1\text{AR-EYFP}$  molecules decrease total density, its brightness remains the same (coefficient of variation: 3.81%), while  $\beta_1\text{AR-2xEYFP}$  exhibits declining brightness (coefficient of variance: 29.43%) and reached the

monomeric brightness. Four different membrane regions corresponding to the same spots within each frame was analyzed and obtained brightness-density values were averaged. Black and blue lines connect data points. Each data point is the mean  $\pm$  SD of three independent experiments. **(E and F)** Data was implemented from Figure 2B. Scatter dot plot representing the oligomeric states **(E)** between 0-30 receptors per  $\mu\text{m}^2$  resulted in average brightness values for  $\beta_1\text{AR-EYFP}$ :  $1.01 \pm 0.08$ ,  $\beta_1\text{AR-2xYEFP}$ :  $1.97 \pm 0.12$  and  $\text{CXCR4-EYFP}$ :  $1.42 \pm 0.21$ , and **(F)** between 85-150 receptors  $\beta_1\text{AR-EYFP}$ :  $1.01 \pm 0.12$ ,  $\beta_1\text{AR-2xYEFP}$ :  $2.04 \pm 0.13$  and  $\text{CXCR4-EYFP}$ :  $2.14 \pm 0.19$  (mean  $\pm$  SD). Each data point represents the calculated oligomeric state from a single cell. **(G)** Density-dependence of brightness for SNAP-CXCR4 and SNAP- $\beta_1\text{AR}$  expressed and imaged in HEK293AD cells. **(H)** Brightness measurement of the controls and CXCR4-EYFP in CHO-K1 cells, plotted as a function of receptor density.

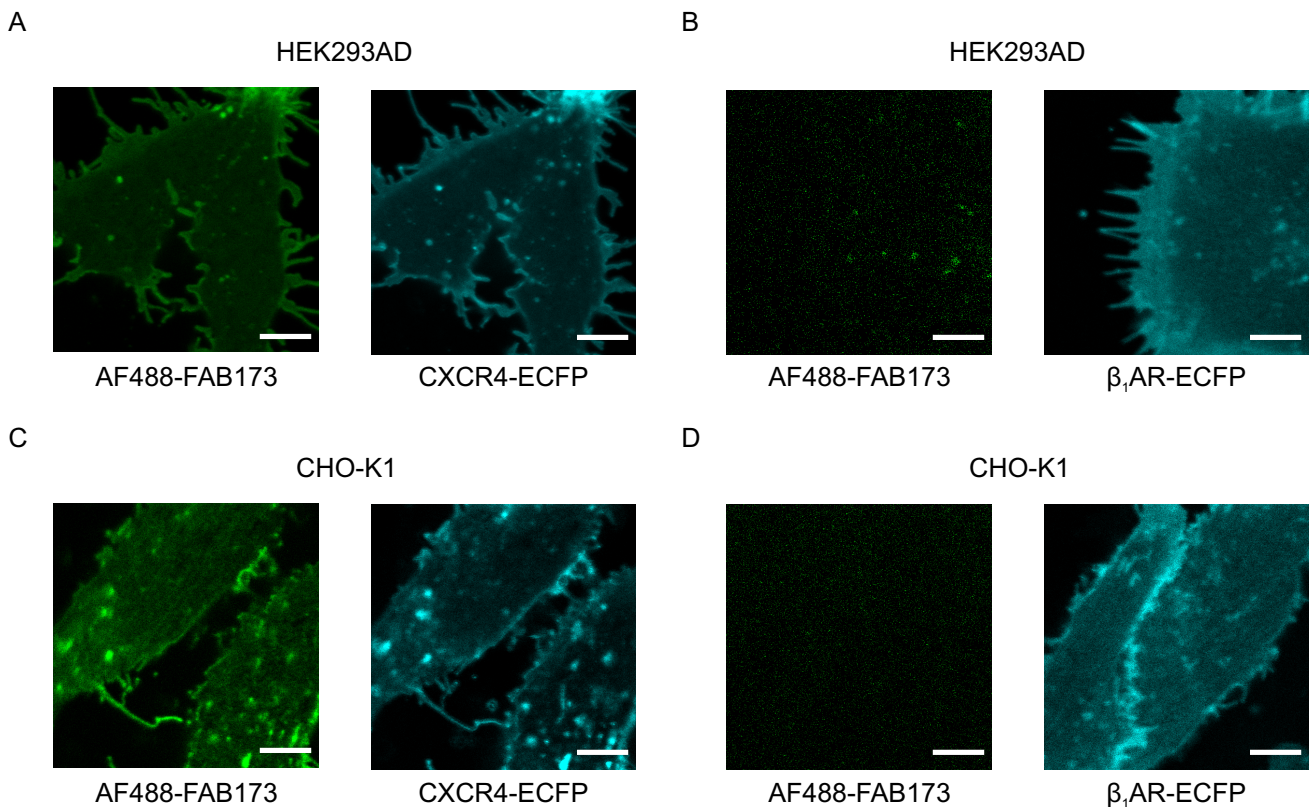


**Figure S3: Immunocytochemistry based assessment of endogenous CXCR4 expression in HEK293AD and CHO-K1 cells.** Cells were transfected with CXCR4-ECFP (A and C) or  $\beta_1$ AR-ECFP (B and D) and then were labeled with the AlexaFluor488 labeled CXCR4 antibody (FAB173G). Image acquisition settings used for SpIDA was employed. In CXCR4-ECFP overexpressing cells, the antibody detected the CXCR4 epitope (A and C, green channel). In  $\beta_1$ AR-ECFP expressing cells, no analyzable fluorescent signal was detected in the green channel, indicating that CXCR4 expression was below the detection levels of SpIDA (i.e. below 5 receptors/ $\mu\text{m}^2$  membrane area (3,500 receptors/cell). Images are representative of 3 independent immunocytochemistry experiments. Scale bar (white): 5 $\mu\text{m}$ .

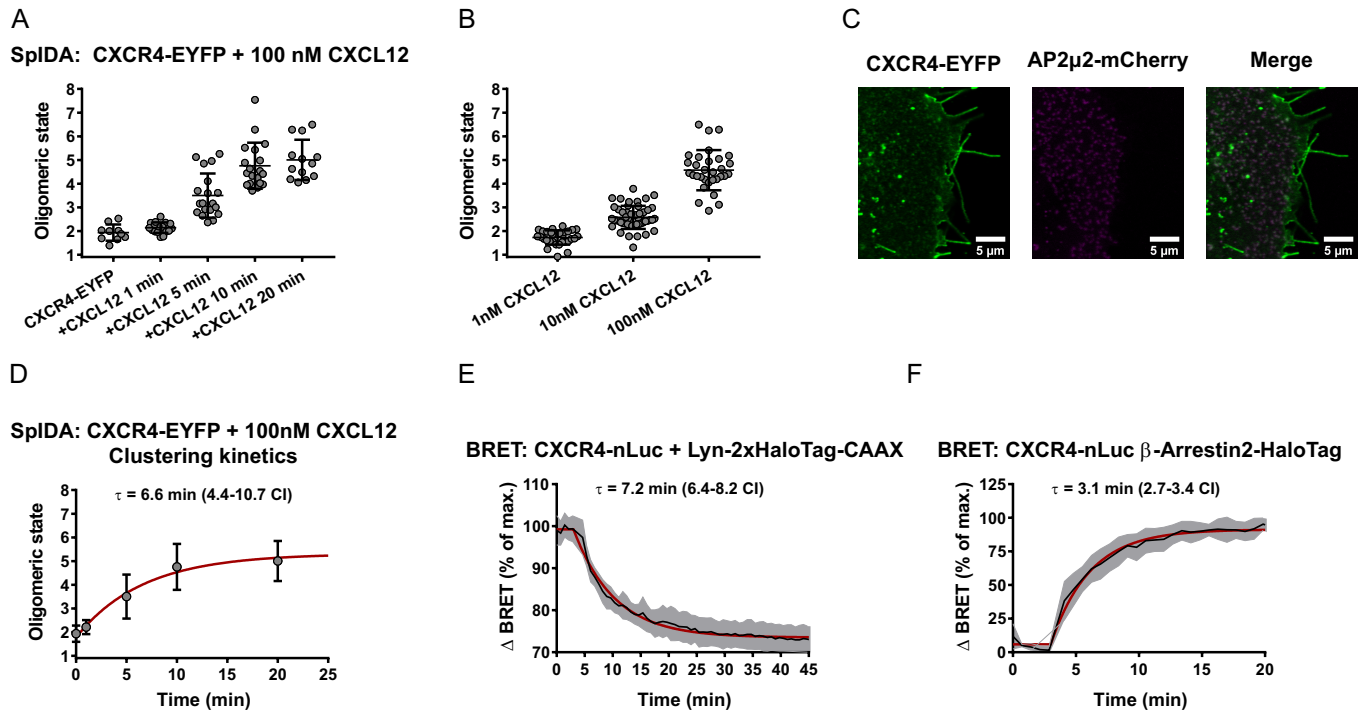


**Figure S4: Agonist-mediated clustering of CXCR4.** (A and B) SpIDA-based brightness measurement of CXCR4-EYFP as a time-course with 100 nM CXCL12 (A) and effect of different concentrations of CXCL12 measured after 20 minutes of ligand exposure (B). Each data point represents monomer-normalized brightness value obtained from a single cell. Data is shown with mean  $\pm$  SD. (C) Representative confocal microscopy image of CXCR4-EYFP and AP2μ2-mCherry after 20 min exposure to 100 nM CXCL12. Merge image displays colocalization of CXCR4 clusters with AP2μ2. (D) Kinetic representation of CXCR4 clustering via CXCL12. Each data point represents the mean  $\pm$  SD of the data in S4A. (E and F) Kinetic BRET measurement of β-arrestin2 recruitment (E) and receptor internalization (F) after stimulation with 100 nM CXCL12. Data is shown as mean (black curves)  $\pm$  SD (gray shades) from 3 independent plate reader experiments (D, E and F). Tau values were obtained by fitting an “exponential decay followed by plateau” function (red curves).

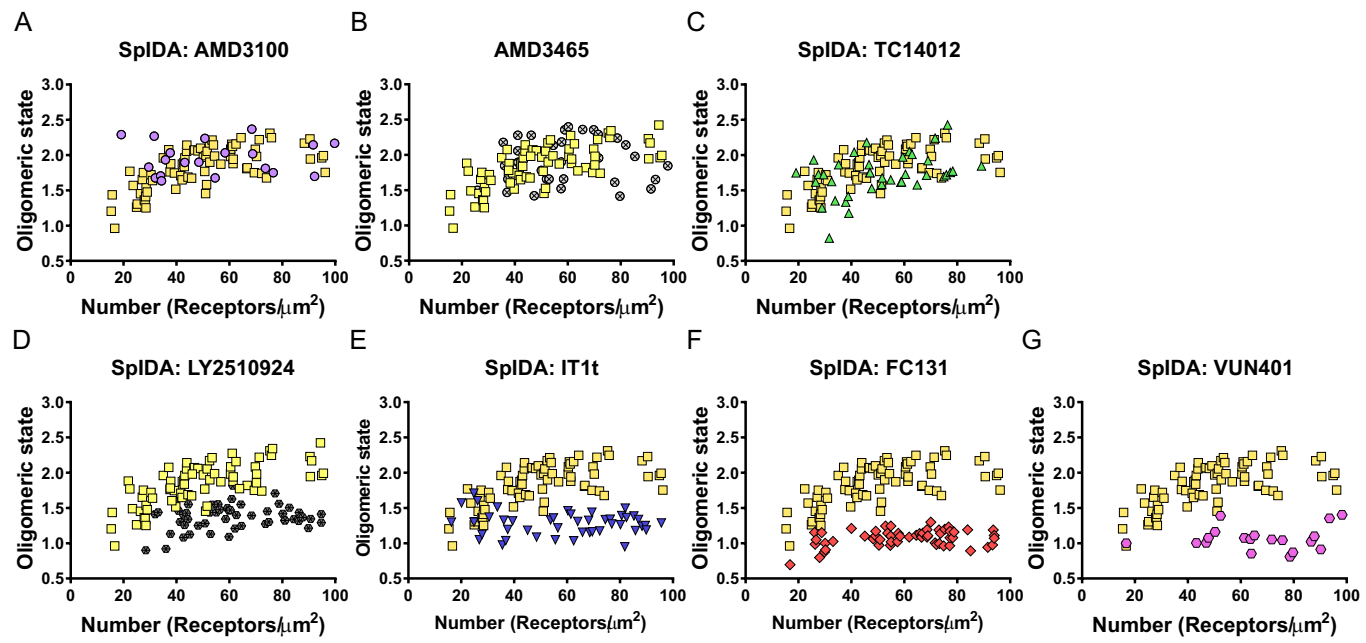


**Figure S5: Density dependence of CXCR4-EYFP brightness under antagonist treatment.** (A-E) Normalized brightness values from cells expressing CXCR4-EYFP and treated with 10 $\mu$ M AMD3100 (A) and 10 $\mu$ M AMD3465 (B), 10 $\mu$ M TC14012 (C), 100nM LY2510924 (D), 10 $\mu$ M IT1t (E), 10 $\mu$ M FC131 (F), and 10 $\mu$ M VUN401 (G). Each data point represents the monomer control-normalized brightness value from single cells.

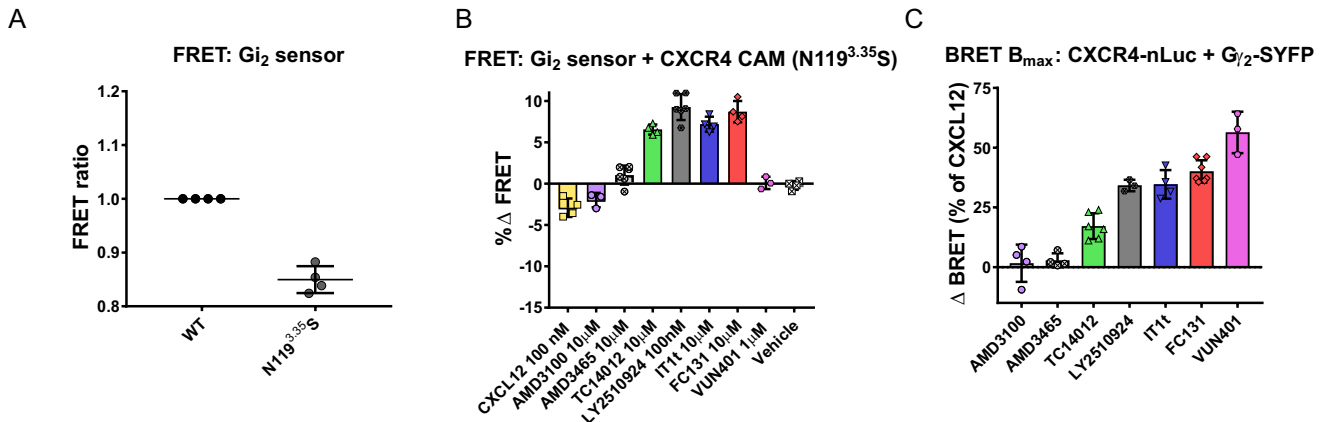


**Figure S6: Assessment of  $\text{Gi}$  protein activation by CAM CXCR4 ( $\text{N}119^{3,35}\text{S}$ ) and WT CXCR4-G protein interactions.** **(A)** Data points represent FRET ratios of  $\text{Gi}_2$  FRET sensor co-expressed with either WT CXCR4 (black) or CAM CXCR4 (grey) and normalized to the data from WT CXCR4 of the same plate.  $\text{N}119^{3,35}\text{S}$  mutant mediates higher basal activity of  $\text{Gi}_2$  protein than WT CXCR4, as it displays a lower FRET ratio at basal state. **(B)** Measurement of  $\text{Gi}$  activation by CAM CXCR4 using the  $\text{Gi}_2$  FRET sensor with different CXCR4 ligands. Scatter dot plots with bars represent ligand mediated FRET change (mean  $\pm$  SD) relative to basal in mean with SD of at least 3 different plate reader experiments. Statistical significance analyses are given in Supplementary Table 2. **(C)** Bar graph representing maximal CXCR4-nLuc+ $\text{G}_{\alpha 2}$ -SYFP BRET responses induced by CXCR4 antagonist. BRET changes (mean  $\pm$  SD) (normalized for each experiment to the maximum response observed by 100 nM CXCL12) with the highest concentrations of the ligands in Fig. 4B. Statistical significance analysis is provided in Supplementary Table 3.

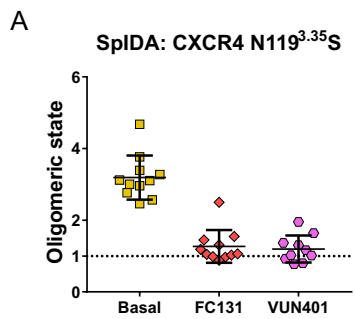


**Figure S7: Oligomerization analysis of the CAM CXCR4 (N119<sup>3.35</sup>S) variant. (A)** SpIDA results of the CXCR4- N119<sup>3.35</sup>S –EYFP variant at basal (yellow) and overnight treatment with 10 $\mu$ M FC131 or (red) 1 $\mu$ M VUN401 (pink and dark pink) treatment.

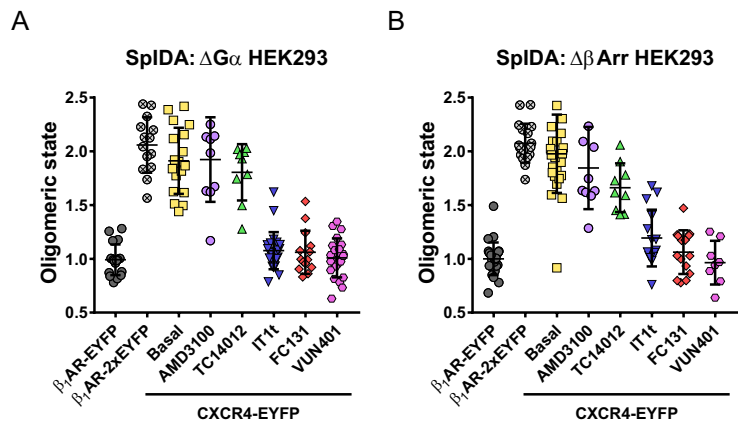


**Figure S8: Oligomerization analysis of CXCR4-EYFP in cells lacking functional  $G\alpha$  subunits or  $\beta$ -arrestins.** SpIDA in HEK293 cells devoid of  $G\alpha$  subunits (A) or  $\beta$ -arrestin1/2 (B). Analyzed are  $\beta_1\text{AR-EYFP}$ ,  $\beta_1\text{AR-2xEYFP}$  and CXCR4-EYFP at basal level or post-exposure to the ligands for 20 minutes at concentrations given in Fig. 5A. Each dataset is given with mean  $\pm$  SD.

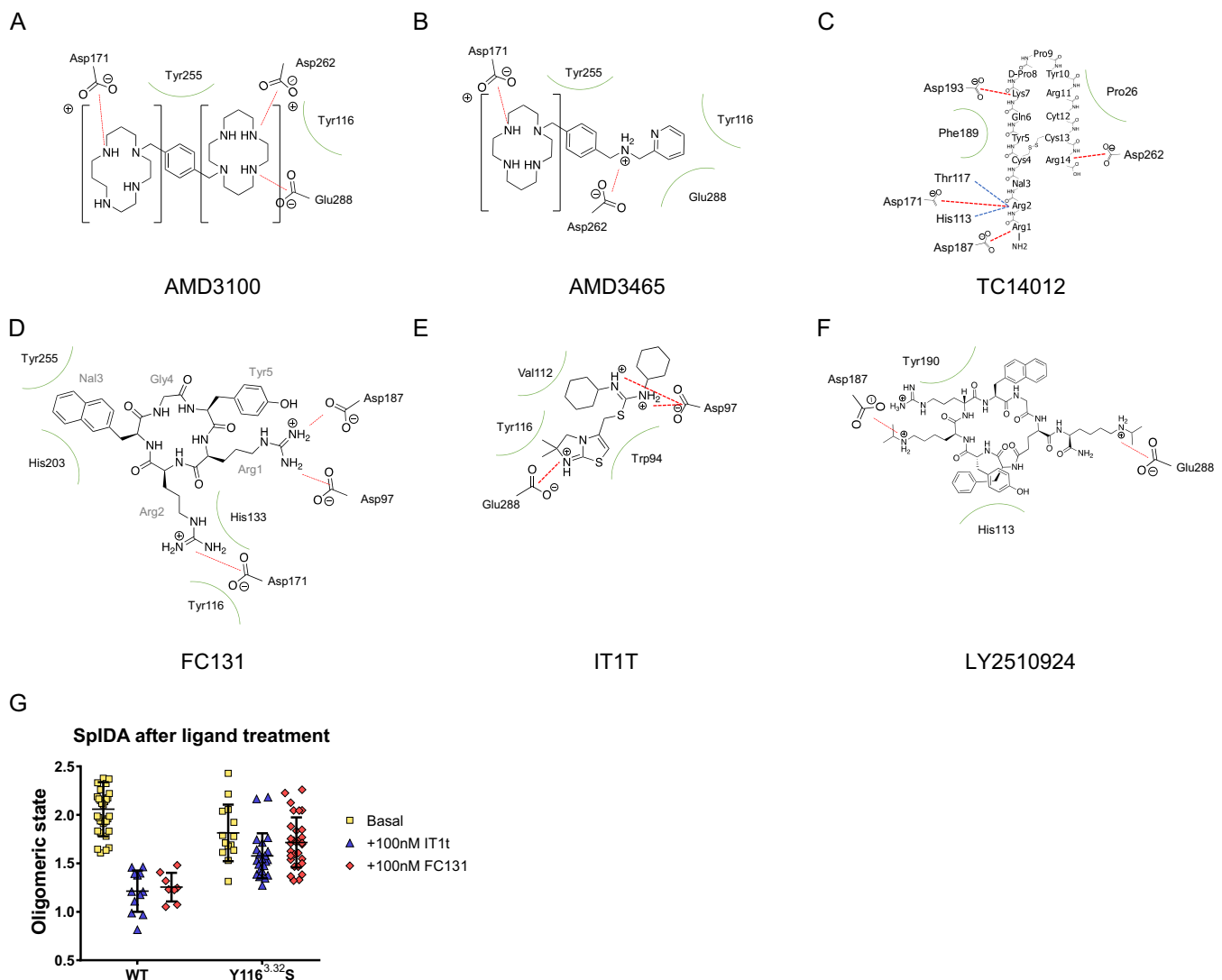


**Figure S9: 2-D maps of ligand receptor interactions.** (A-F) Ligand-receptor interaction sites as retrieved from docking. Each residue of CXCR4 (shown in red) that is in contact with the ligands is shown with their specific interaction types. Ionic interactions between residues and ligand atoms are shown with red lines, and hydrophobic interactions are shown as green arches. (G) SpIDA analysis of the WT CXCR4 and Y116<sup>3.32S</sup> variant (yellow), after 20 minutes of incubation 100 nM IT1t (blue) and 10  $\mu$ M FC131 (red). Each data point represents a brightness value from one cell normalized to the monomer control, given with mean  $\pm$  SD as error bars. Data were obtained from at least 3 experiments per condition.

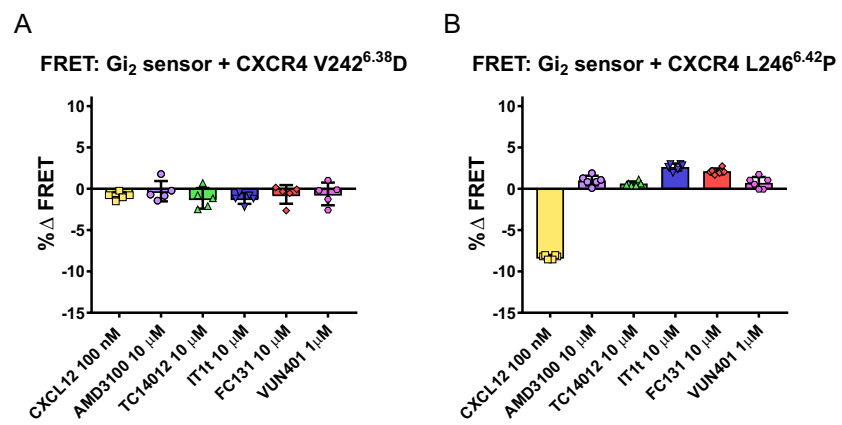


**Figure S10: Assessment of  $\text{Gi}_2$  protein activation by CXCR4 ligands on TM6 mutants.**  
Measurement of  $\text{Gi}$  activation by CAM CXCR4 using the  $\text{Gi}_2$  FRET sensor with different CXCR4 ligands for the  $\text{V}242^{6,38}\text{D}$  (**A**) and the  $\text{L}246^{6,42}\text{P}$  (**B**) mutants of the CXCR4. Scatter dot plots with bars represent ligand-mediated FRET change (mean  $\pm$  SD) relative to basal in mean with SD of at least 3 different plate reader experiments.

**Table S1: Multiple comparison and significance test results for Figure 3A.**

Tukey's multiple comparisons test	Mean Diff,	95,00% CI of diff,	Significant?	Summary	Adjusted P Value
$\beta_1$ AR-EYFP vs. Basal	-1,03	-1,192 to -0,8672	Yes	****	<0,0001
$\beta_1$ AR-EYFP vs. CXCL12	-1,158	-1,335 to -0,9817	Yes	****	<0,0001
$\beta_1$ AR-EYFP vs. IT1t	-0,2771	-0,4309 to -0,1233	Yes	****	<0,0001
$\beta_1$ AR-EYFP vs. FC131	-0,112	-0,2565 to 0,03244	No	ns	0,2860
$\beta_1$ AR-EYFP vs. AMD3100	-0,991	-1,19 to -0,7917	Yes	****	<0,0001
$\beta_1$ AR-EYFP vs. TC14012	-0,8694	-1,043 to -0,6954	Yes	****	<0,0001
$\beta_1$ AR-EYFP vs. VUN401	-0,07642	-0,2504 to 0,09752	No	ns	0,9250
$\beta_1$ AR-EYFP vs. AMD3465	-0,981	-1,167 to -0,795	Yes	****	<0,0001
$\beta_1$ AR-EYFP vs. LY2510924	-0,4226	-0,5809 to -0,2644	Yes	****	<0,0001
Basal vs. CXCL12	-0,1286	-0,3003 to 0,04306	No	ns	0,3343
Basal vs. IT1t	0,7525	0,6042 to 0,9008	Yes	****	<0,0001
Basal vs. FC131	0,9176	0,779 to 1,056	Yes	****	<0,0001
Basal vs. AMD3100	0,03857	-0,1565 to 0,2336	No	ns	0,9998
Basal vs. TC14012	0,1602	-0,008794 to 0,3293	No	ns	0,0796
Basal vs. VUN401	0,9532	0,7841 to 1,122	Yes	****	<0,0001
Basal vs. AMD3465	0,04859	-0,1328 to 0,23	No	ns	0,9975
Basal vs. LY2510924	0,607	0,4541 to 0,7598	Yes	****	<0,0001
CXCL12 vs. IT1t	0,8811	0,7175 to 1,045	Yes	****	<0,0001
CXCL12 vs. FC131	1,046	0,8913 to 1,201	Yes	****	<0,0001
CXCL12 vs. AMD3100	0,1672	-0,0398 to 0,3742	No	ns	0,2327
CXCL12 vs. TC14012	0,2889	0,1062 to 0,4716	Yes	****	<0,0001
CXCL12 vs. VUN401	1,082	0,8991 to 1,264	Yes	****	<0,0001
CXCL12 vs. AMD3465	0,1772	-0,01696 to 0,3714	No	ns	0,1071
CXCL12 vs. LY2510924	0,7356	0,5678 to 0,9034	Yes	****	<0,0001
IT1t vs. FC131	0,1651	0,03663 to 0,2935	Yes	**	0,0022
IT1t vs. AMD3100	-0,7139	-0,9019 to -0,5259	Yes	****	<0,0001
IT1t vs. TC14012	-0,5923	-0,7531 to -0,4314	Yes	****	<0,0001
IT1t vs. VUN401	0,2007	0,03983 to 0,3615	Yes	**	0,0035
IT1t vs. AMD3465	-0,7039	-0,8777 to -0,5301	Yes	****	<0,0001
IT1t vs. LY2510924	-0,1455	-0,2893 to -0,001813	Yes	*	0,0444
FC131 vs. AMD3100	-0,879	-1,059 to -0,6985	Yes	****	<0,0001
FC131 vs. TC14012	-0,7573	-0,9093 to -0,6054	Yes	****	<0,0001
FC131 vs. VUN401	0,03563	-0,1163 to 0,1876	No	ns	0,9991
FC131 vs. AMD3465	-0,869	-1,035 to -0,7034	Yes	****	<0,0001
FC131 vs. LY2510924	-0,3106	-0,4443 to -0,1769	Yes	****	<0,0001
AMD3100 vs. TC14012	0,1217	-0,08312 to 0,3265	No	ns	0,6699
AMD3100 vs. VUN401	0,9146	0,7098 to 1,119	Yes	****	<0,0001
AMD3100 vs. AMD3465	0,01003	-0,2051 to 0,2251	No	ns	>0,9999
AMD3100 vs. LY2510924	0,5684	0,3768 to 0,76	Yes	****	<0,0001
TC14012 vs. VUN401	0,7929	0,6127 to 0,9731	Yes	****	<0,0001
TC14012 vs. AMD3465	-0,1117	-0,3035 to 0,08018	No	ns	0,6958
TC14012 vs. LY2510924	0,4467	0,2816 to 0,6118	Yes	****	<0,0001
VUN401 vs. AMD3465	-0,9046	-1,096 to -0,7128	Yes	****	<0,0001
VUN401 vs. LY2510924	-0,3462	-0,5113 to -0,1811	Yes	****	<0,0001
AMD3465 vs. LY2510924	0,5584	0,3807 to 0,7361	Yes	****	<0,0001

Test details	Mean 1	Mean 2	Mean Diff,	SE of diff,	n1	n2	q	DF
$\beta_1$ AR-EYFP vs. Basal	0,9836	2,013	-1,03	0,0508	22	25	28,66	225
$\beta_1$ AR-EYFP vs. CXCL12	0,9836	2,142	-1,158	0,05524	22	18	29,65	225
$\beta_1$ AR-EYFP vs. IT1t	0,9836	1,261	-0,2771	0,04813	22	32	8,142	225
$\beta_1$ AR-EYFP vs. FC131	0,9836	1,096	-0,112	0,04521	22	45	3,505	225
$\beta_1$ AR-EYFP vs. AMD3100	0,9836	1,975	-0,991	0,06237	22	12	22,47	225
$\beta_1$ AR-EYFP vs. TC14012	0,9836	1,853	-0,8694	0,05443	22	19	22,59	225
$\beta_1$ AR-EYFP vs. VUN401	0,9836	1,06	-0,07642	0,05443	22	19	1,986	225
$\beta_1$ AR-EYFP vs. AMD3465	0,9836	1,965	-0,981	0,05819	22	15	23,84	225
$\beta_1$ AR-EYFP vs. LY2510924	0,9836	1,406	-0,4226	0,04951	22	28	12,07	225
Basal vs. CXCL12	2,013	2,142	-0,1286	0,05372	25	18	3,386	225
Basal vs. IT1t	2,013	1,261	0,7525	0,04639	25	32	22,94	225
Basal vs. FC131	2,013	1,096	0,9176	0,04335	25	45	29,93	225
Basal vs. AMD3100	2,013	1,975	0,03857	0,06103	25	12	0,8936	225
Basal vs. TC14012	2,013	1,853	0,1602	0,05289	25	19	4,284	225
Basal vs. VUN401	2,013	1,06	0,9532	0,05289	25	19	25,48	225
Basal vs. AMD3465	2,013	1,965	0,04859	0,05676	25	15	1,211	225
Basal vs. LY2510924	2,013	1,406	0,607	0,04782	25	28	17,95	225
CXCL12 vs. IT1t	2,142	1,261	0,8811	0,0512	18	32	24,34	225
CXCL12 vs. FC131	2,142	1,096	1,046	0,04847	18	45	30,53	225
CXCL12 vs. AMD3100	2,142	1,975	0,1672	0,06477	18	12	3,651	225
CXCL12 vs. TC14012	2,142	1,853	0,2889	0,05716	18	19	7,147	225
CXCL12 vs. VUN401	2,142	1,06	1,082	0,05716	18	19	26,76	225
CXCL12 vs. AMD3465	2,142	1,965	0,1772	0,06076	18	15	4,125	225
CXCL12 vs. LY2510924	2,142	1,406	0,7356	0,0525	18	28	19,81	225
IT1t vs. FC131	1,261	1,096	0,1651	0,04019	32	45	5,808	225
IT1t vs. AMD3100	1,261	1,975	-0,7139	0,05883	32	12	17,16	225
IT1t vs. TC14012	1,261	1,853	-0,5923	0,05033	32	19	16,64	225
IT1t vs. VUN401	1,261	1,06	0,2007	0,05033	32	19	5,639	225
IT1t vs. AMD3465	1,261	1,965	-0,7039	0,05438	32	15	18,3	225
IT1t vs. LY2510924	1,261	1,406	-0,1455	0,04497	32	28	4,577	225
FC131 vs. AMD3100	1,096	1,975	-0,879	0,05646	45	12	22,02	225
FC131 vs. TC14012	1,096	1,853	-0,7573	0,04755	45	19	22,52	225
FC131 vs. VUN401	1,096	1,06	0,03563	0,04755	45	19	1,06	225
FC131 vs. AMD3465	1,096	1,965	-0,869	0,05182	45	15	23,72	225
FC131 vs. LY2510924	1,096	1,406	-0,3106	0,04183	45	28	10,5	225
AMD3100 vs. TC14012	1,975	1,853	0,1217	0,06408	12	19	2,685	225
AMD3100 vs. VUN401	1,975	1,06	0,9146	0,06408	12	19	20,18	225
AMD3100 vs. AMD3465	1,975	1,965	0,01003	0,06731	12	15	0,2106	225
AMD3100 vs. LY2510924	1,975	1,406	0,5684	0,05996	12	28	13,41	225
TC14012 vs. VUN401	1,853	1,06	0,7929	0,05639	19	19	19,89	225
TC14012 vs. AMD3465	1,853	1,965	-0,1117	0,06003	19	15	2,631	225
TC14012 vs. LY2510924	1,853	1,406	0,4467	0,05166	19	28	12,23	225
VUN401 vs. AMD3465	1,06	1,965	-0,9046	0,06003	19	15	21,31	225
VUN401 vs. LY2510924	1,06	1,406	-0,3462	0,05166	19	28	9,479	225
AMD3465 vs. LY2510924	1,965	1,406	0,5584	0,05561	15	28	14,2	225

**Table S2: Multiple comparison and significance test results for Figure 4A and S6B**

**WT CXCR4**

Tukey's multiple comparisons test	Mean Diff,	95.00% CI of diff,	Significant?	Summary	Adjusted P Value
CXCL12 100 nM vs. AMD3100 10µM	-12,39	-13,94 to -10,83	Yes	****	<0,0001
CXCL12 100 nM vs. TC14012 10µM	-13,82	-15,21 to -12,43	Yes	****	<0,0001
CXCL12 100 nM vs. IT1t 10µM	-16,02	-17,33 to -14,72	Yes	****	<0,0001
CXCL12 100 nM vs. FC131 10µM	-16,15	-17,54 to -14,76	Yes	****	<0,0001
CXCL12 100 nM vs. VUN401 1µM	-12,34	-13,8 to -10,88	Yes	****	<0,0001
CXCL12 100 nM vs. Vehicle	-12,2	-13,59 to -10,81	Yes	****	<0,0001
CXCL12 100 nM vs. AMD3465 10µM	-13,03	-14,42 to -11,64	Yes	****	<0,0001
CXCL12 100 nM vs. LY2510924 100nM	-15,19	-16,49 to -13,89	Yes	****	<0,0001
AMD3100 10µM vs. TC14012 10µM	-1,432	-2,986 to 0,1233	No	ns	0,0930
AMD3100 10µM vs. IT1t 10µM	-3,637	-5,112 to -2,162	Yes	****	<0,0001
AMD3100 10µM vs. FC131 10µM	-3,766	-5,321 to -2,211	Yes	****	<0,0001
AMD3100 10µM vs. VUN401 1µM	0,04596	-1,57 to 1,662	No	ns	>0,9999
AMD3100 10µM vs. Vehicle	0,1917	-1,363 to 1,747	No	ns	>0,9999
AMD3100 10µM vs. AMD3465 10µM	-0,6396	-2,194 to 0,9152	No	ns	0,9141
AMD3100 10µM vs. LY2510924 100nM	-2,799	-4,274 to -1,324	Yes	****	<0,0001
TC14012 10µM vs. IT1t 10µM	-2,205	-3,506 to -0,9044	Yes	****	<0,0001
TC14012 10µM vs. FC131 10µM	-2,334	-3,725 to -0,9437	Yes	****	<0,0001
TC14012 10µM vs. VUN401 1µM	1,477	0,01891 to 2,936	Yes	*	0,0450
TC14012 10µM vs. Vehicle	1,623	0,2325 to 3,014	Yes	*	0,0116
TC14012 10µM vs. AMD3465 10µM	0,7919	-0,5988 to 2,183	No	ns	0,6481
TC14012 10µM vs. LY2510924 100nM	-1,368	-2,669 to -0,06705	Yes	*	0,0325
IT1t 10µM vs. FC131 10µM	-0,1291	-1,43 to 1,172	No	ns	>0,9999
IT1t 10µM vs. VUN401 1µM	3,683	2,31 to 5,056	Yes	****	<0,0001
IT1t 10µM vs. Vehicle	3,828	2,528 to 5,129	Yes	****	<0,0001
IT1t 10µM vs. AMD3465 10µM	2,997	1,696 to 4,298	Yes	****	<0,0001
IT1t 10µM vs. LY2510924 100nM	0,8373	-0,367 to 2,042	No	ns	0,3853
FC131 10µM vs. VUN401 1µM	3,812	2,353 to 5,27	Yes	****	<0,0001
FC131 10µM vs. Vehicle	3,958	2,567 to 5,348	Yes	****	<0,0001
FC131 10µM vs. AMD3465 10µM	3,126	1,736 to 4,517	Yes	****	<0,0001
FC131 10µM vs. LY2510924 100nM	0,9664	-0,3344 to 2,267	No	ns	0,2994
VUN401 1µM vs. Vehicle	0,1457	-1,313 to 1,604	No	ns	>0,9999
VUN401 1µM vs. AMD3465 10µM	-0,6856	-2,144 to 0,773	No	ns	0,8358
VUN401 1µM vs. LY2510924 100nM	-2,845	-4,219 to -1,472	Yes	****	<0,0001
Vehicle vs. AMD3465 10µM	-0,8313	-2,222 to 0,5594	No	ns	0,5876
Vehicle vs. LY2510924 100nM	-2,991	-4,292 to -1,69	Yes	****	<0,0001
AMD3465 10µM vs. LY2510924 100nM	-2,16	-3,461 to -0,8589	Yes	****	<0,0001

Test details	Mean 1	Mean 2	Mean Diff,	SE of diff,	n1	n2	q	DF
CXCL12 100 nM vs. AMD3100 10µM	-12,21	0,1758	-12,39	0,4779	6	4	36,66	46
CXCL12 100 nM vs. TC14012 10µM	-12,21	1,607	-13,82	0,4274	6	6	45,72	46
CXCL12 100 nM vs. IT1t 10µM	-12,21	3,813	-16,02	0,3998	6	8	56,68	46
CXCL12 100 nM vs. FC131 10µM	-12,21	3,942	-16,15	0,4274	6	6	53,45	46
CXCL12 100 nM vs. VUN401 1µM	-12,21	0,1298	-12,34	0,4483	6	5	38,93	46
CXCL12 100 nM vs. Vehicle	-12,21	-0,01588	-12,2	0,4274	6	6	40,35	46
CXCL12 100 nM vs. AMD3465 10µM	-12,21	0,8154	-13,03	0,4274	6	6	43,1	46
CXCL12 100 nM vs. LY2510924 100nM	-12,21	2,975	-15,19	0,3998	6	8	53,72	46
AMD3100 10µM vs. TC14012 10µM	0,1758	1,607	-1,432	0,4779	4	6	4,236	46
AMD3100 10µM vs. IT1t 10µM	0,1758	3,813	-3,637	0,4533	4	8	11,34	46
AMD3100 10µM vs. FC131 10µM	0,1758	3,942	-3,766	0,4779	4	6	11,14	46
AMD3100 10µM vs. VUN401 1µM	0,1758	0,1298	0,04596	0,4966	4	5	0,1309	46
AMD3100 10µM vs. Vehicle	0,1758	-0,01588	0,1917	0,4779	4	6	0,5672	46
AMD3100 10µM vs. AMD3465 10µM	0,1758	0,8154	-0,6396	0,4779	4	6	1,893	46
AMD3100 10µM vs. LY2510924 100nM	0,1758	2,975	-2,799	0,4533	4	8	8,733	46
TC14012 10µM vs. IT1t 10µM	1,607	3,813	-2,205	0,3998	6	8	7,8	46
TC14012 10µM vs. FC131 10µM	1,607	3,942	-2,334	0,4274	6	6	7,724	46
TC14012 10µM vs. VUN401 1µM	1,607	0,1298	1,477	0,4483	6	5	4,661	46
TC14012 10µM vs. Vehicle	1,607	-0,01588	1,623	0,4274	6	6	5,371	46
TC14012 10µM vs. AMD3465 10µM	1,607	0,8154	0,7919	0,4274	6	6	2,62	46
TC14012 10µM vs. LY2510924 100nM	1,607	2,975	-1,368	0,3998	6	8	4,839	46
IT1t 10µM vs. FC131 10µM	3,813	3,942	-0,1291	0,3998	8	6	0,4567	46
IT1t 10µM vs. VUN401 1µM	3,813	0,1298	3,683	0,422	8	5	12,34	46
IT1t 10µM vs. Vehicle	3,813	-0,01588	3,828	0,3998	8	6	13,54	46
IT1t 10µM vs. AMD3465 10µM	3,813	0,8154	2,997	0,3998	8	6	10,6	46
IT1t 10µM vs. LY2510924 100nM	3,813	2,975	0,8373	0,3702	8	8	3,199	46
FC131 10µM vs. VUN401 1µM	3,942	0,1298	3,812	0,4483	6	5	12,03	46
FC131 10µM vs. Vehicle	3,942	-0,01588	3,958	0,4274	6	6	13,09	46
FC131 10µM vs. AMD3465 10µM	3,942	0,8154	3,126	0,4274	6	6	10,34	46
FC131 10µM vs. LY2510924 100nM	3,942	2,975	0,9664	0,3998	6	8	3,418	46
VUN401 1µM vs. Vehicle	0,1298	-0,01588	0,1457	0,4483	5	6	0,4596	46
VUN401 1µM vs. AMD3465 10µM	0,1298	0,8154	-0,6856	0,4483	5	6	2,163	46
VUN401 1µM vs. LY2510924 100nM	0,1298	2,975	-2,845	0,422	5	8	9,535	46
Vehicle vs. AMD3465 10µM	-0,01588	0,8154	-0,8313	0,4274	6	6	2,751	46
Vehicle vs. LY2510924 100nM	-0,01588	2,975	-2,991	0,3998	6	8	10,58	46
AMD3465 10µM vs. LY2510924 100nM	0,8154	2,975	-2,16	0,3998	6	8	7,64	46

## CAM CXCR4

Tukey's multiple comparisons test	Mean Diff,	95,00% CI of diff,	Significant?	Summary	Adjusted P Value
CXCL12 100 nM vs. AMD3100 10µM	-0,9164	-3,716 to 1,883	No	ns	0,9703
CXCL12 100 nM vs. TC14012 10µM	-9,449	-12,04 to -6,858	Yes	****	<0,0001
CXCL12 100 nM vs. IT1t 10µM	-10,09	-12,68 to -7,501	Yes	****	<0,0001
CXCL12 100 nM vs. FC131 10µM	-11,62	-14,21 to -9,025	Yes	****	<0,0001
CXCL12 100 nM vs. VUN401 1µM	-2,995	-5,794 to -0,1954	Yes	*	0,0290
CXCL12 100 nM vs. Vehicle	-2,689	-5,28 to -0,09713	Yes	*	0,0374
CXCL12 100 nM vs. AMD3465 10µM	-3,938	-6,303 to -1,572	Yes	***	0,0002
CXCL12 100 nM vs. LY2510924 100nM	-12,17	-14,53 to -9,802	Yes	****	<0,0001
AMD3100 10µM vs. TC14012 10µM	-8,533	-11,33 to -5,734	Yes	****	<0,0001
AMD3100 10µM vs. IT1t 10µM	-9,176	-11,98 to -6,377	Yes	****	<0,0001
AMD3100 10µM vs. FC131 10µM	-10,7	-13,5 to -7,901	Yes	****	<0,0001
AMD3100 10µM vs. VUN401 1µM	-2,078	-5,071 to 0,9143	No	ns	0,3613
AMD3100 10µM vs. Vehicle	-1,772	-4,571 to 1,027	No	ns	0,4811
AMD3100 10µM vs. AMD3465 10µM	-3,021	-5,613 to -0,4296	Yes	*	0,0132
AMD3100 10µM vs. LY2510924 100nM	-11,25	-13,84 to -8,66	Yes	****	<0,0001
TC14012 10µM vs. IT1t 10µM	-0,6436	-3,235 to 1,948	No	ns	0,9948
TC14012 10µM vs. FC131 10µM	-2,167	-4,758 to 0,4245	No	ns	0,1593
TC14012 10µM vs. VUN401 1µM	6,455	3,656 to 9,254	Yes	****	<0,0001
TC14012 10µM vs. Vehicle	6,761	4,169 to 9,352	Yes	****	<0,0001
TC14012 10µM vs. AMD3465 10µM	5,512	3,146 to 7,877	Yes	****	<0,0001
TC14012 10µM vs. LY2510924 100nM	-2,719	-5,084 to -0,353	Yes	*	0,0152
IT1t 10µM vs. FC131 10µM	-1,523	-4,115 to 1,068	No	ns	0,5764
IT1t 10µM vs. VUN401 1µM	7,098	4,299 to 9,897	Yes	****	<0,0001
IT1t 10µM vs. Vehicle	7,404	4,813 to 9,996	Yes	****	<0,0001
IT1t 10µM vs. AMD3465 10µM	6,155	3,79 to 8,521	Yes	****	<0,0001
IT1t 10µM vs. LY2510924 100nM	-2,075	-4,441 to 0,2906	No	ns	0,1214
FC131 10µM vs. VUN401 1µM	8,622	5,823 to 11,42	Yes	****	<0,0001
FC131 10µM vs. Vehicle	8,928	6,336 to 11,52	Yes	****	<0,0001
FC131 10µM vs. AMD3465 10µM	7,679	5,313 to 10,04	Yes	****	<0,0001
FC131 10µM vs. LY2510924 100nM	-0,5517	-2,917 to 1,814	No	ns	0,9966
VUN401 1µM vs. Vehicle	0,3059	-2,493 to 3,105	No	ns	>0,9999
VUN401 1µM vs. AMD3465 10µM	-0,943	-3,534 to 1,649	No	ns	0,9459
VUN401 1µM vs. LY2510924 100nM	-9,173	-11,76 to -6,582	Yes	****	<0,0001
Vehicle vs. AMD3465 10µM	-1,249	-3,615 to 1,117	No	ns	0,7023
Vehicle vs. LY2510924 100nM	-9,479	-11,84 to -7,114	Yes	****	<0,0001
AMD3465 10µM vs. LY2510924 100nM	-8,23	-10,35 to -6,114	Yes	****	<0,0001

Test details	Mean 1	Mean 2	Mean Diff,	SE of diff,	n1	n2	q	DF
CXCL12 100 nM vs. AMD3100 10 $\mu$ M	-2,91	-1,993	-0,9164	0,8366	4	3	1,549	29
CXCL12 100 nM vs. TC14012 10 $\mu$ M	-2,91	6,54	-9,449	0,7745	4	4	17,25	29
CXCL12 100 nM vs. IT1t 10 $\mu$ M	-2,91	7,183	-10,09	0,7745	4	4	18,43	29
CXCL12 100 nM vs. FC131 10 $\mu$ M	-2,91	8,707	-11,62	0,7745	4	4	21,21	29
CXCL12 100 nM vs. VUN401 1 $\mu$ M	-2,91	0,08496	-2,995	0,8366	4	3	5,062	29
CXCL12 100 nM vs. Vehicle	-2,91	-0,221	-2,689	0,7745	4	4	4,909	29
CXCL12 100 nM vs. AMD3465 10 $\mu$ M	-2,91	1,028	-3,938	0,707	4	6	7,876	29
CXCL12 100 nM vs. LY2510924 100nM	-2,91	9,258	-12,17	0,707	4	6	24,34	29
AMD3100 10 $\mu$ M vs. TC14012 10 $\mu$ M	-1,993	6,54	-8,533	0,8366	3	4	14,42	29
AMD3100 10 $\mu$ M vs. IT1t 10 $\mu$ M	-1,993	7,183	-9,176	0,8366	3	4	15,51	29
AMD3100 10 $\mu$ M vs. FC131 10 $\mu$ M	-1,993	8,707	-10,7	0,8366	3	4	18,09	29
AMD3100 10 $\mu$ M vs. VUN401 1 $\mu$ M	-1,993	0,08496	-2,078	0,8943	3	3	3,286	29
AMD3100 10 $\mu$ M vs. Vehicle	-1,993	-0,221	-1,772	0,8366	3	4	2,996	29
AMD3100 10 $\mu$ M vs. AMD3465 10 $\mu$ M	-1,993	1,028	-3,021	0,7745	3	6	5,516	29
AMD3100 10 $\mu$ M vs. LY2510924 100nM	-1,993	9,258	-11,25	0,7745	3	6	20,54	29
TC14012 10 $\mu$ M vs. IT1t 10 $\mu$ M	6,54	7,183	-0,6436	0,7745	4	4	1,175	29
TC14012 10 $\mu$ M vs. FC131 10 $\mu$ M	6,54	8,707	-2,167	0,7745	4	4	3,957	29
TC14012 10 $\mu$ M vs. VUN401 1 $\mu$ M	6,54	0,08496	6,455	0,8366	4	3	10,91	29
TC14012 10 $\mu$ M vs. Vehicle	6,54	-0,221	6,761	0,7745	4	4	12,34	29
TC14012 10 $\mu$ M vs. AMD3465 10 $\mu$ M	6,54	1,028	5,512	0,707	4	6	11,02	29
TC14012 10 $\mu$ M vs. LY2510924 100nM	6,54	9,258	-2,719	0,707	4	6	5,438	29
IT1t 10 $\mu$ M vs. FC131 10 $\mu$ M	7,183	8,707	-1,523	0,7745	4	4	2,782	29
IT1t 10 $\mu$ M vs. VUN401 1 $\mu$ M	7,183	0,08496	7,098	0,8366	4	3	12	29
IT1t 10 $\mu$ M vs. Vehicle	7,183	-0,221	7,404	0,7745	4	4	13,52	29
IT1t 10 $\mu$ M vs. AMD3465 10 $\mu$ M	7,183	1,028	6,155	0,707	4	6	12,31	29
IT1t 10 $\mu$ M vs. LY2510924 100nM	7,183	9,258	-2,075	0,707	4	6	4,151	29
FC131 10 $\mu$ M vs. VUN401 1 $\mu$ M	8,707	0,08496	8,622	0,8366	4	3	14,57	29
FC131 10 $\mu$ M vs. Vehicle	8,707	-0,221	8,928	0,7745	4	4	16,3	29
FC131 10 $\mu$ M vs. AMD3465 10 $\mu$ M	8,707	1,028	7,679	0,707	4	6	15,36	29
FC131 10 $\mu$ M vs. LY2510924 100nM	8,707	9,258	-0,5517	0,707	4	6	1,103	29
VUN401 1 $\mu$ M vs. Vehicle	0,08496	-0,221	0,3059	0,8366	3	4	0,5172	29
VUN401 1 $\mu$ M vs. AMD3465 10 $\mu$ M	0,08496	1,028	-0,943	0,7745	3	6	1,722	29
VUN401 1 $\mu$ M vs. LY2510924 100nM	0,08496	9,258	-9,173	0,7745	3	6	16,75	29
Vehicle vs. AMD3465 10 $\mu$ M	-0,221	1,028	-1,249	0,707	4	6	2,498	29
Vehicle vs. LY2510924 100nM	-0,221	9,258	-9,479	0,707	4	6	18,96	29
AMD3465 10 $\mu$ M vs. LY2510924 100nM	1,028	9,258	-8,23	0,6324	6	6	18,41	29

**Table S3: Statistical outlier analysis and of the linear fit on Figure 4C:**

Straight line	
Best-fit values	
YIntercept	0,9528
Slope	0,01112
Std. Error	
YIntercept	0,03084
Slope	0,0004855
95% CI (profile likelihood)	
YIntercept	0,8919 to 1,014
Slope	0,01016 to 0,01208
Goodness of Fit	
Degrees of Freedom	158
R square	0,7686
Absolute Sum of Squares	5,946
Sy.x	0,194
Number of points	
# of X values	179
# Y values analyzed	179
Outliers (excluded, Q=1%)	1